Urea Induced Unfolding Dynamics of Flavin Adenine Dinucleotide (FAD): Spectroscopic and Molecular Dynamics Simulation Studies from Femto-Second to Nanosecond Regime

ARTICLE *in* THE JOURNAL OF PHYSICAL CHEMISTRY B · JANUARY 2014

Impact Factor: 3.3 · DOI: 10.1021/jp412339a · Source: PubMed

THE JOURNAL OF PHYSICAL CHEMISTRY B

Article

pubs.acs.org/JPCB

Urea Induced Unfolding Dynamics of Flavin Adenine Dinucleotide (FAD): Spectroscopic and Molecular Dynamics Simulation Studies from Femto-Second to Nanosecond Regime

Abhigyan Sengupta,[†] Reman K. Singh,[†] Krishna Gavvala, Raj Kumar Koninti, Arnab Mukherjee,* and Partha Hazra*

Department of Chemistry, Indian Institute of Science Education and Research (IISER)-Pune, Pune (411008), Maharashtra, India

Supporting Information

ABSTRACT: Here, we investigate the effect of urea in the unfolding dynamics of flavin adenine dinucleotide (FAD), an important enzymatic cofactor, through steady state, time-resolved fluorescence spectroscopic and molecular dynamics (MD) simulation studies. Steady state results indicate the possibility of urea induced unfolding of FAD, inferred from increasing emission intensity of FAD with urea. The TCSPC and up-conversion results suggest that the stack−unstack dynamics of FAD severely gets affected in the presence of urea and leads to an increase in the unstack conformation population from 15% in pure water to 40% in 12 M urea. Molecular dynamics simulation was employed to understand the nature of the interaction between FAD and urea at the molecular level. Results depict that urea molecules replace many of the water molecules around adenine and isoalloxazine rings of FAD. However, the major driving force for the stability of this unstack conformations arises from the favorable stacking interaction of a significant fraction of the urea molecules with adenine and isoalloxazine rings of FAD, which overcomes the intramolecular stacking interaction between themselves observed in pure water.

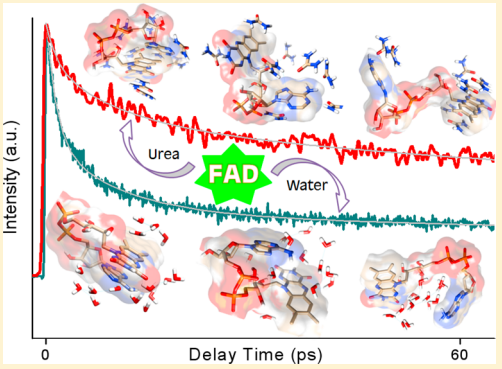

INTRODUCTION

Light induced behavior of living organisms is mainly controlled by five enzymatic cofactors, namely, carotinoids, billins, chlorophyls, pterins, and flavins. Out of these, flavins received greater attention from several decades because of its ubiquitous existence in flavoproteins and important role in catalyzing a number of single or two electron redox reactions.[1−4] Among others (namely, flavin mononucleotide (FMN) and riboflavin (RF)), FAD shares a special importance as a photoreceptor due to its existence in a wide variety of photoactive flavoproteins such as DNA-photolyase, BLUF, and cryptochromes.[5−8] The photophysical properties of FAD is a continual center of attention for a prolonged duration since Weber reported a remarkably weak fluorescence of FAD ($\Phi_f \sim 0.03$) in water compared to RF and FMN ($\Phi_f \sim 0.3$).[9] All these flavin cofactors contain a fluorescent isoalloxazine (flavin) ring and a ribityl side chain. Unlike others, FAD along with isoalloxazine and ribityl chain contains an adenosine moiety linked by a phosphodiester group (Scheme 1), which acts as an intrinsic quencher for isoalloxazine fluorescence. The simultaneous existence of a fluorescent (isoalloxazine) and a quencher moiety (adenine) in FAD attributes unique structural dynamics of FAD in water exhibiting three distinct conformations, "stack" (or closed) and "unstack" (or open), along with an intermediate conformation named as "partially stack".[10−12] It is also reported that the dominant contribution of stack conformation of FAD in water (80%) results low fluorescence quantum yield[9,10] due to the combined effects of static and

Scheme 1. Molecular Structures of FAD and FMN

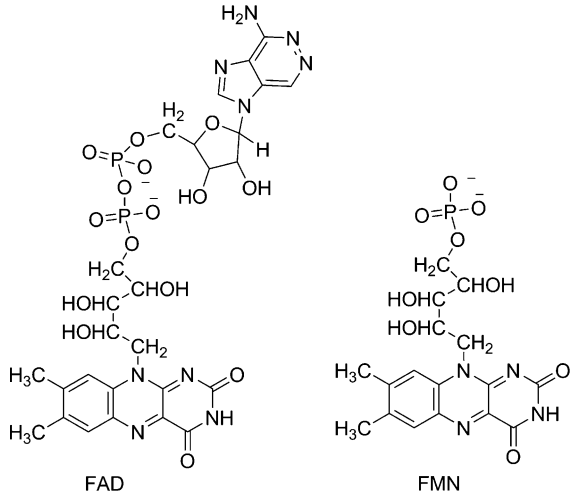

Received: December 17, 2013
Revised: January 23, 2014
Published: January 23, 2014

   dx.doi.org/10.1021/jp412339a | J. Phys. Chem. B 2014, 118, 1881−1890

dynamic quenching of flavin ring by the adenine moiety.[10,11,13,14]

FAD being one of the most important cofactors for electron transportation and photoreceptors in living systems,[5−8] the photophysical properties of FAD have been extensively studied to date.[10,11,14−19] It is established that FAD shows three distinct lifetime components at physiological pH; a ∼10 ps component is detected from stack conformation, a ∼2.2 ns lifetime appears from partially stack conformation, and ∼4 ns component originates from "open" conformation.[10,11] Recently, a ∼4 ps decaying component attributed to the stack conformation was reported from the transient absorption and up-conversion studies.[13,16] Moreover, time-resolved mid-IR transient absorption study shows a radical recombination dynamics of ∼1.1 ps along with a stack dynamics of ∼9 ps of FAD at higher concentrations in D_2O.[15] Ernsting and co-workers presented a detailed vibrational analysis based on hybrid density functional theory for riboflavin in the first excited state (S_1) and FAD in the ground state (S_0) using normal-mode analysis and resonance Raman.[17] Recently, it has been observed that the stacking dynamics of FAD in solution is largely affected by the surrounding environment. In ethanol−water mixture, lowering of dielectric constant increases the contribution of unstack conformation of FAD. Moreover, the fluorescence lifetime of the stacked conformation also increases with decreasing dielectric constant, suggesting an increasing intramolecular distance between the two aromatic rings in less dielectric media.[20] Furthermore, the study on the glycerol−water mixture suggests that viscosity affects the lifetime of only the "open" conformation of FAD.[20] A more detailed insight about the stacking dynamics of FAD in a methanol−water mixture is offered by Gutman et al. through molecular dynamics simulation along with experiments for the same system. Interestingly, the results claim that the effect of methanol on the equilibrium is to destabilize the folded state of FAD, enhancing the contribution of the "open" conformations.[18,19] Overall, it concludes the solvent-dependent folding observed for FAD appears due to solvent−solute interactions.[18,19] Very recently, we noticed dependence of FAD dynamics over the solvent polarity and viscosity inside the reverse micelles.[21] Now, based on such a diverse collection of literatures, it appears difficult to pinpoint the factor(s) that is (are) responsible for folding dynamics of FAD. Stacking interaction between adenine and flavin might contribute significantly toward the stabilization of stack form of FAD. Recent simulation studies predicted the hydrogen bonds between phosphodiester and ribityl chain as a possible reason for dominating percentage of stack conformation in water.[11,18,19] These ongoing quests about FAD folding dynamics fascinated us to pursue a thorough investigation to find out the role of stacking and/or hydrogen bond interactions in the FAD dynamics in urea, as it is widely accepted as chaotrope for creating chaos in hydrogen networked systems[22−25] and it is also well-known for unfolding protein structures.[26−28] To do so, we have employed picoseconds time-resolved (TCSPC) and femtosecond fluorescence up-conversion techniques, along with long (200 ns) molecular dynamics simulations to study FAD in urea−water mixture and compared that with the dynamics of FAD in pure water. Our study captures both the dynamics and the structural aspects of FAD in the presence of urea and provides the molecular origin of unfolding.

EXPERIMENTAL SECTION

Reagents, Methods, and Instrumentations. FAD (HPLC grade, purity ≥96%) was purchased from Sigma Aldrich, and FMN was bought from Fluka (HPLC grade, purity ∼90%). Urea (Biochemical grade) was procured from Sigma Aldrich. For all steady state fluorescence experiments, the concentration of FAD and FMN was kept low at $\sim 10 \times 10^{-6}$ M to avoid the effect of molecular aggregation. Urea concentration was varied form 0 to 12 M respectively. All samples were prepared in Millipore water. Freshly prepared and properly equilibrated solutions were used for each set of data collection. Experimental temperature was kept at 298 K, unless otherwise specified.

Absorption measurements were performed on UV-2600 absorption spectrophotometer (Shimadzu) and steady state fluorescence spectra were collected in FluoroMax-4 spectrofluorimeter (Horiba Scientific, U.S.A.). We have taken into account the dilution effect due to solid urea addition, and dilution corrected emission spectra are shown in the manuscript. Fluorescence lifetime and time-resolved anisotropy measurements were collected by time-correlated single photon counting (TCSPC) setup from IBH Horiba Jobin Yvon (U.S.A.) using 440 nm diode laser. The detailed description of the instrument is mentioned elsewhere.[29−32] The analysis of lifetime and anisotropy data is done by IBH DAS6 analysis software. We fitted lifetime and anisotropy data with a minimum number of exponentials. Quality of each fitting was judged by χ^2 values and the visual inspection of the residuals where value of $\chi^2 \approx 1$ was considered as best fit for the plots. Error in TCSPC measurements obtained from our results is ∼5%.

The detail of femtosecond upconversion setup (FOG 100, CDP) is described in our previous report.[33] The sample was excited at 420 nm using the second harmonic of a mode-locked Ti-sapphire laser (Mai-Tai, Spectra Physics). The 840 nm fundamental beam was frequency doubled in a nonlinear crystal and the emitted fluorescence from sample was upconverted in another nonlinear crystal using the gated pulse of the fundamental beam. The sum frequency of fluorescence and the gate pulse was detected as a function of the time delay between excitation and gate pulses. The angle between the polarization of the pump and gate pulses was kept at magic angle (54.7°) to eliminate effects from rotational diffusion. The up-converted signal is dispersed in a monochromator and detected using photon counting electronics. A cross-correlation function obtained using the Raman scattering from ethanol displayed a full-width at half-maximum (fwhm) of ∼350 fs. Error in up-conversion measurements obtained from our results is ∼15%.

Simulation Method. FAD was optimized quantum mechanically using HF/6-31G* basis set in GAUSSIAN03 software.[34] Further, restricted electrostatic potential (resp) charges on the atoms of FAD were calculated using ANTECHAMBER module of AMBER11 software.[35,36] The general amber force field (GAFF)[37] for flavin adenine dinucleotide (FAD) and urea was constructed using AmberTools software.[35] The topology and coordinates generated from AmberTools were converted into GROMACS format using a perl program amb2gmx.pl.[38] Following two systems were created for subsequent study: (i) FAD in water only and (ii) FAD in water−urea mixture. To create the FAD−water system, FAD was solvated with 2581 TIP3P water

dx.doi.org/10.1021/jp412339a | J. Phys. Chem. B 2014, 118, 1881−1890

molecules[39] in a cubic box of dimension 42.8 Å. To create FAD−water−urea system, 372 urea molecules and 2581 TIP3P water molecules were added to FAD to make 8 M urea solution. Additionally, two sodium ions were added to neutralize the system.

Both the systems were taken through usual equilibration processes. All the simulations were performed using molecular dynamics software GROMACS.[40] First, each system was minimized using the steepest descent[41] method, followed by heating to 300 K in 100 ps by using Berendsen thermostat[42] with a coupling constant of 0.2 ps. During the heating process, a harmonic restraint of 25 kcal/mol was applied to the heavy atoms of FAD. The harmonic restraint was gradually reduced to 0.25 kcal/mol in six steps. In each step, 100 ps equilibration was carried out at constant temperature (300 K) and pressure (1 bar) using Berendsen thermostat and barostat[42] with coupling constants of 0.2 ps each. This was then followed by energy minimization using the steepest descent method.[41] All bonds were constrained using LINCS algorithm.[43] Particle Mesh Ewald (PME) method[44] was used for the electrostatics with a 10 Å cutoff for the long-range interaction. Cut-off for the van der Waals (vdW) interaction was kept at 10 Å. Simulations were performed by 1 fs time step. At the final equilibration step, we performed the 1 ns unrestrained equilibration by using the Berendsen thermostat and barostat[21] with a coupling constant of 0.2 ps each.

After the equilibration steps, a final unrestrained simulation of 200 ns was performed at constant temperature 300 K and constant pressure 1 bar using the Nose-Hoover thermostat[45] and Parrinello-Rahman barostat,[46] respectively, with 0.2 ps coupling constant for each. Results reported here were obtained from this final simulation.

RESULTS AND DISCUSSIONS

Steady State Results. Flavin absorption in water is characterized by two intense $\pi-\pi^*$ transition bands originated from isoalloxazine chromophore corresponding to $S_0 \rightarrow S_1$ transition ($\lambda_{abs} \sim 450$ nm) and $S_0 \rightarrow S_2$ transition ($\lambda_{abs} \sim 375$ nm).[10,47] When excited at either of the absorption bands, both FMN and FAD in water exhibit an unstructured emission at ~535 nm (Figure 1).[10,47] With the incremental addition of urea to the solution containing FMN (devoid of adenine moiety), emission exhibits almost negligible effect. Interestingly, on gradual addition of urea to the solution containing FAD, the fluorescence intensity is enhanced more than double of its initial value at maximum urea concentration (12 M). It is reported that increasing urea concentration in water enhances the dielectric of the medium,[48] which is expected to stabilize the stack conformation of FAD.[18−20] We observed, however, a completely opposite trend for FAD intensity in presence of urea. Hence, the modulation of photophysics observed either for FAD or FMN in presence of urea is surely not an outcome of dielectric variation of the medium. The quenching witnessed for FMN may be attributed to the alteration of hydrogen bonding network with surrounding solvents in presence of urea, as it is already evident that urea can break hydrogen bonds between solute and water, and itself gets involved in hydrogen bond interaction with the solute molecules.[22−25,49,50] The difference in fluorescence property between FMN and FAD in presence of urea thus arises due to the existence of adenine moiety in FAD, which is absent in case of FMN. Notably, adenine participates in the formation of weakly fluorescent stack conformation with flavin ring through photoinduced

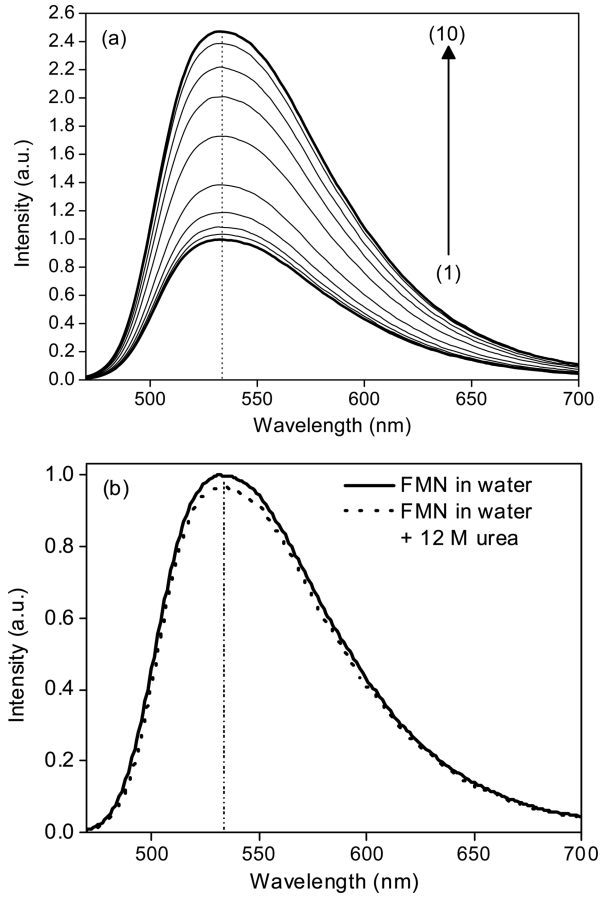

Figure 1. Emission profiles of (a) FAD with increasing concentration of urea where, (1) → (10) represents concentrations of urea 0, 0.25, 0.5, 1, 2, 4, 6, 8, 10, and 12 M, respectively, and (b) FMN in water and in presence of urea.

intramolecular electron transfer process.[10,11,13,20] Here it is relevant to mention that the fluorescence property of the unstack conformation is believed to be similar to that of FMN, as the latter appears solely from the isoalloxazine ring. Hence, we believe that the unstack conformation of FAD would also experience similar quenching as that of FMN even though we have observed continuous increment in emission intensity in presence of urea. Above observations suggests that there are two opposing factors that affect FAD fluorescence in presence of urea; however, the effect of enhancement dominates over the effect of quenching. The observed enhancement in fluorescence intensity is certainly due to the increased population of the unstack conformation of FAD, as the stack conformation is almost nonfluorescent in nature. This is corroborated by the molecular picture obtained from the all-atom simulation, as mentioned later. Therefore, we believe that urea affects the stacking interaction between adenine and isoalloxazine ring and shifts the equilibrium toward the unstack conformation. A more detailed insight of interaction between flavin and urea can be obtained from the time-resolved as well as the molecular dynamics simulation studies discussed afterward.

Pico-Second to Nanosecond Time-Resolved Decay Features of FAD with Increasing Urea Concentration. Figure 2 depicts fluorescence decays of FMN and FAD collected using TCSPC technique and the results are tabulated in Table 1. It is evident from the decay profiles that FMN exhibits single exponential decay in the absence and presence of

dx.doi.org/10.1021/jp412339a | J. Phys. Chem. B 2014, 118, 1881−1890

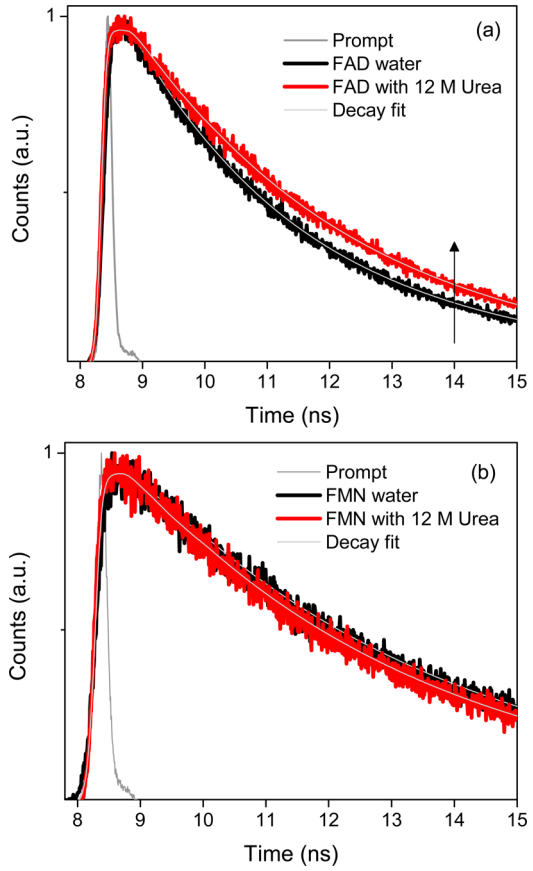

Figure 2. Time resolved decay profiles (measured in TCSPC setup, λ_{ex} = 440 nm and λ_{em} = 535 nm) of (a) FAD and (b) FMN water and in the presence of urea. The legends carry the respective meanings.

urea, as it does not have any conformational flexibility. Lifetime of FMN is almost unchanged in the presence of urea. This indicates that the dynamics of FMN is almost unaffected by the presence of urea, which is corroborative with the steady state results. The decay characteristics of FAD in the absence and presence of urea is biexponential in nature. The longest decaying lifetime component (4.6 ns) of FAD is already known to appear from unstack conformation of FAD, and in good correlation with the single decaying component of FMN (Figure 2, Table 1). The short nanosecond component (~2.5 ns) is assigned to be the lifetime of partially stack conformation of FAD.[10] It is noticeable that lifetime of unstack conformation reduces slightly from bulk water to 10 M urea (Table 1). This clearly implies that like FMN the unstack conformation of FAD also suffers the effect of quenching in the presence of urea. The effect of decreasing lifetime component is attributed to the change of hydrogen bonding network by urea. However, in steady state emission spectra, we could not observe this quenching effect as the enhancement dominates over quenching. From the TCSPC results, we also infer that the population of unstack conformation increases, whereas the percentage contribution of partially stack conformation decreases (Table 1), resulting in a marginal increase in the average lifetime. Note that TCSPC study cannot probe the dynamics of stack conformation of FAD due to the limited time resolution of the setup. To probe the stacking dynamics of FAD in the presence of urea, we employed femtosecond fluorescence up-conversion technique, discussed in the forthcoming section.

Femtosecond Time-Resolved Decay Features of FAD with Increasing Urea Concentration. The femtosecond decay profiles are depicted in Figure 3. The results are summarized in Table 2. All the femtosecond decay profiles are nonexponential in nature. We have used a tetra exponential fit function to fit the decay profiles of FAD.

$$I(t) = A_1 \exp\left(-\frac{t}{\tau_1}\right) + A_2 \exp\left(-\frac{t}{\tau_2}\right) + A_3 \exp\left(-\frac{t}{\tau_3}\right) + A_4 \exp\left(-\frac{t}{\tau_4}\right) \quad (1)$$

where A_i and τ_i represent the pre-exponential factor (reflecting the contribution of i^{th} species in the decay profile) and lifetime of i^{th} species, respectively. From the fitting of the decay profile of FAD in water alone, we have obtained 1.5, ~10, and 200 ps lifetime components, which we have assigned as τ_1, τ_2, and τ_3, respectively. These lifetime components are in agreement with previous reports.[10,11,20] The 1.5 ps component is ascribed to solvent relaxation around FAD, which is yet to be completed.[10,20] The major point of attention is the appearance of two of the lifetime components, ~10 and ~200 ps. The ~10 ps component is attributed to the stack conformation, where the isoalloxazine and the adenine moieties residing within stacking distance (distance between center of mass of the two rings <5.5 Å[18,19]) participate in an effective electron transfer process, which results in minimal fluorescence lifetime among all the conformations. Another picosecond decaying component (~200 ps) is in good agreement with ~220 ps component reported previously by Visser et al.[11] and Ohta et al.[20] This component was attributed to another type of stack con-

Table 1. Fluorescence Lifetime Decay Parameters (Collected at 535 nm in TCSPC Set-Up) of FAD and FMN in Water and the Presence of Urea

	FAD						FMN		
sample	τ_1 (ns)	a_1 (%)	τ_2 (ns)	a_2 (%)	χ^2	τ_{av} (ns)	τ_1 (ns)	a	χ^2
urea 0 M	2.32	47	4.62	53	0.95	3.54	4.98	100	1.15
urea 0.5 M	2.37	46	4.62	54	0.95	3.58	4.82	100	1.10
urea 1 M	2.46	56	4.62	44	0.99	3.41	4.76	100	1.18
urea 2 M	2.60	59	4.65	41	1.10	3.44	4.74	100	0.95
urea 4 M	2.85	64	4.60	36	1.10	3.48	4.72	100	1.00
urea 6 M	3.06	70	4.60	30	0.95	3.78	4.65	100	1.13
urea 8 M	3.32	67	4.60	33	0.85	3.74	4.63	100	1.00
urea 10 M	3.42	72	4.62	28	1.00	3.75	4.62	100	1.13
urea 12 M	3.52	73	4.62	27	0.99	3.82	4.62	100	1.10

dx.doi.org/10.1021/jp412339a | J. Phys. Chem. B 2014, 118, 1881−1890

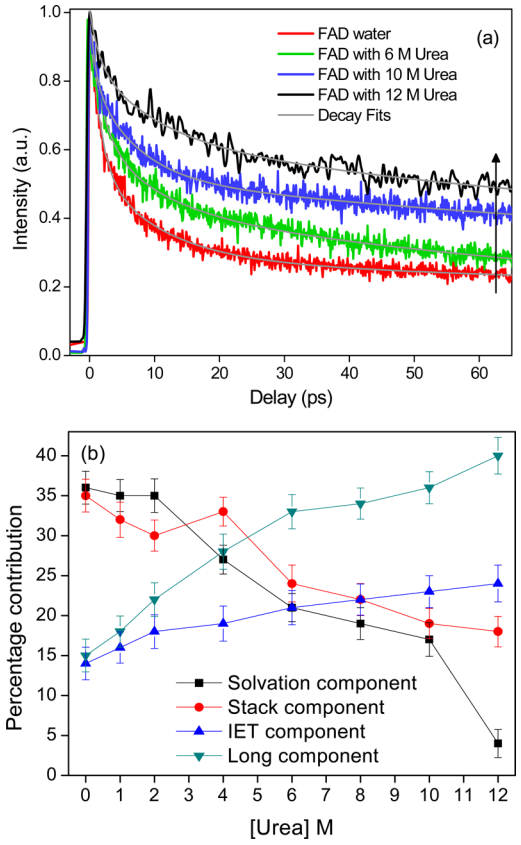

Figure 3. Femtosecond time-resolved decay profiles of FAD and FMN (λ_{ex} = 420 nm and λ_{em} = 535 nm) in water and with increasing concentrations of urea up to 12 M. (b) Changes in percentage contribution in femtosecond decay components with variable urea concentrations. In all cases, the legends carry respective meanings.

Table 2. Fitting Parameters of Femtosecond Time-Resolved Fluorescence Decays of FAD in Water and with Increasing Concentrations of Urea

sample	τ_1 (ps)	A_1 (%)	τ_2 (ps)	A_2 (%)	τ_3 (ps)	A_3 (%)	τ_4 (ps)	A_4 (%)
FAD water	1	36	12	35	212	14	3500	15
FAD + urea 1 M	1	35	12	32	180	16	3500	18
FAD + urea 2 M	1	35	12	30	162	18	3500	22
FAD + urea 4 M	1	27	12	33	97	19	3500	28
FAD + urea 6 M	1	21	12	24	104	21	3500	33
FAD + urea 8 M	1	19	12	22	95	22	3500	34
FAD + urea 10 M	1	17	10	19	84	23	3500	36
FAD + urea 12 M	1	4	12	18	130	24	3500	40

formation where the intramolecular electron transfer (IET) is relatively less effective due to slightly higher distance between flavin and adenine rings. Here it is pertinent to mention that the oxidation potential of adenine (E_{ox} = 1.5 eV)[51] allows the electron transfer from adenine to photoexcited flavin ring (ground state reduction potential E_{red} = −0.24 eV),[52] resulting in a reduced fluorescence lifetime of the flavin ring. This intramolecular electron transfer (IET) process is largely dependent over the distances between two rings. The existence of stack conformation is strongly supported by the FMN decay profile, which is devoid of any such picosecond components, as it lacks the adenine moiety (Figure 3 and Table 2). The long component lifetime (τ_4, detected in TCSPC) is assigned to the average lifetime of "open" and partially stack conformations of FAD and kept fixed during analysis. The analysis of all the decay profiles in the presence of urea are fitted with the assumption that the same fast-decaying components having a lifetime of 1.5 (τ_1) and ∼10 ps (τ_2) exist in the presence of urea with variable contribution and the long component lifetime (τ_4) obtained from TCSPC is also kept fixed during analysis.

It is noticeable from Figure 3 that the residual background having a long decay time increases with the increase in urea concentration. This indicates that the dynamics slows down in presence of urea. The fitting results clearly suggest that the population of solvation component (A_1) gradually decreases as the urea content of the solution increases. Decrease in the contribution of solvation component suggests a limited access of water around the flavin ring with increasing urea concentration. Urea can disrupt the hydrogen bonding interaction; therefore, it is possible that solute−solvent interaction is affected by the presence of urea, which results in the small magnitude of A_1 in the presence of urea. Plots of A_2 and A_3 against urea concentration are shown in Figure 3b. Both A_2 and A_3 represent the value corresponding to the population of stack conformations in solution with different intramolecular distance between adenine and isoalloxazine (flavin) ring. As shown in Table 2, the population of A_2 decreases with increasing urea concentration, indicating a decrease in the population of stack conformation of FAD. Interestingly, the population of stack conformation having lifetime of ∼200 ps in water increases with rise in urea concentration in solution, although its lifetime is getting faster in the presence of urea. This indicates that IET rate also gets affected by the presence of urea. The population of long nanosecond component (A_4) also increases significantly with the increase in urea concentration. These results clearly suggest that urea shifts the equilibrium from the stack toward unstack conformation. Recently, it has been shown by simulation as well as experiments in methanol−water binary mixture that decreasing dielectric constant, lowers the population of stack conformation decreases. It was argued that that methanol affects the dynamics of the FAD by enhancing the frequency of unfolding events without affecting the lifetime of the open conformation.[18,19] Literature reports that dielectric constant of the medium increases with increasing concentration of urea.[48,53] Although an enhanced dielectric constant is well-known to stabilize stack conformation of FAD,[10,18−20] we observe here that the population of stack conformation significantly reduces in presence of urea. Therefore, it is reasonable to conclude that urea itself hampers the stacking interaction between adenine and isoalloxazine ring.

There are two plausible mechanisms by which the stacking interaction in FAD can be hindered. (a) A direct urea induced disruption of intramolecular hydrogen bonding network, which destabilizes stack conformation of FAD and (b) solvation of aromatic moieties (adenine and/or isoalloxazine ring) by urea, which destabilizes the $\pi-\pi$ stacking interaction within FAD. Recently, a few reports showed that urea can severely hinder $\pi-\pi$ stacking interaction by solvating hydrophobic aromatic moieties, like adenine, thymine, and uracil.[26,54] Notably, FAD contains adenine in its structure, which can be easily solvated by urea, thereby creates a hindrance for intramolecular stacking.

dx.doi.org/10.1021/jp412339a | J. Phys. Chem. B 2014, 118, 1881−1890

At the same time, it is well established that urea can interfere with solute−solvent and solvent−solvent, as well as intramolecular hydrogen bonding interaction in a molecule.[22−25] Recent simulation studies on FAD revealed that interplay of hydrogen bond formation between the ribityl chain and the phosphodiester bond might result in the formation of stack and unstack conformations of FAD.[11,18,19] A simulation study also found that there is a possibility of H-bond formation between a hydroxyl group attached to C3/C4 of the ribityl chain and N1 of the flavin in stack conformation.[11] In order to probe the involvement of urea in folding−unfolding dynamics of FAD in molecular detail, we have carried out molecular dynamics simulation study (discussed in the next section). This provides the molecular picture of the interaction in terms of H-bonding and stacking between different parts of FAD and also between FAD and urea, corroborating the observations noted above.

MOLECULAR DYNAMICS SIMULATION

Structure and Dynamics of FAD. Simulation trajectories of 200 ns for each system were used to analyze the conformational sampling of FAD in pure water and water-urea mixture. The following three parameters were used to understand the conformational variations of FAD: (i) distance, d, between the center of masses (COMs) of the adenine (Ade) and isoalloxazine (Iso) rings (magnitude of the vector $\vec{e}$, Figure 4), (ii) angle, θ, between the plane of the Ade and Iso rings (angle between the vectors $\hat{g}$ and $\hat{f}$ in Figure 4), and (iii) angle, φ between the vector normal to the Iso ring and the vector from the COM of Iso to the COM of Ade (angle between two vectors $\hat{f}$ and $\hat{e}$, Figure 4). Stack configuration is defined when $d \leq 6.0$ Å,[18] and both angles (θ and φ) are either less than 40° or greater than 140°, that is, $40° \geq \{\theta, \varphi\}$ or $\{\theta, \varphi\} \geq 140°$, as shown schematically in Figure 4a.

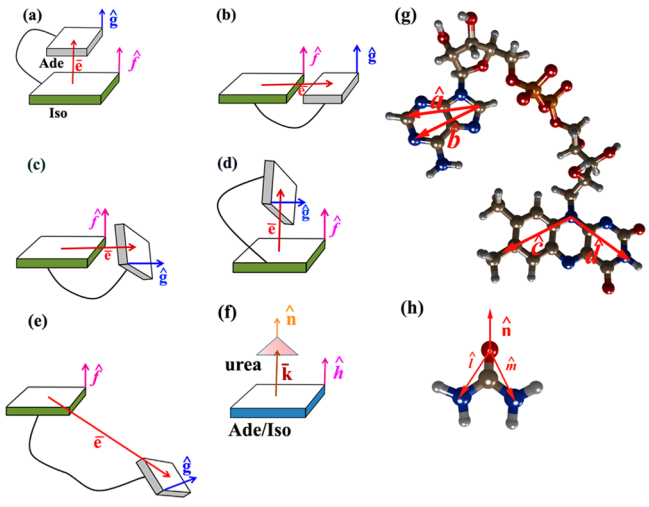

Figure 4. Schematic representation of the stack and unstack conformations: (a) represents the stack conformation, for which $d \leq 6.0$ Å, and $\theta, \varphi = 0°$; (b) represents the unstack conformation, where $d \leq 6.0$ Å, $\theta = 0°$, $\varphi = 90°$; (c) represents the unstack conformation, where $d \leq 6.0$ Å, $\theta = 90°$, $\varphi = 90°$; (d) represents the unstack conformation, where $d \leq 6.0$ Å, $\theta = 90°$, $\varphi = 0°$; (e) represents the unstack conformation, where $d \geq 10$ Å; (f) represents the stack conformation of Ade/Iso with urea when $k \leq 5.2$ Å, $40° \leq \{\alpha, \beta\} \leq 140°$; $\vec{e}$ represents the vector from COM of Iso ring to Ade ring; $\hat{g}$ represents the vector normal to the plane of Ade ring, which is a cross product of two vectors, $\hat{a}$ and $\hat{b}$ (g); $\hat{f}$ represents the vector normal to the plane of Iso ring, which is a cross product of two vectors, $\hat{c}$ and $\hat{d}$ (g); $\hat{n}$ represents the vector normal to the urea molecule, which is a cross product of two vectors, $\hat{l}$ and $\hat{m}$ (h).

We also define the two different types of unstack conformations: (i) complete unstack conformation (U4), where $d > 10$ Å, and (ii) partially unstack, where $d \leq 10$ Å. Based on our observation of the geometry of FAD, we further divide the partially unstacked into three categories: (i) U1, when $d < 6.0$ Å and $40° \leq \{\theta, \varphi\}$ or $\{\theta, \varphi\} \leq 140°$; (ii) U2, when 6 Å $\leq d \leq 10$ Å and $40° \geq \{\theta, \varphi\}$ or $\{\theta, \varphi\} \geq 140°$; (iii) U3, 6 Å $\leq d \leq 10$ Å and $40° \leq \{\theta, \varphi\}$ or $\{\theta, \varphi\} \leq 140°$. U1 denotes the partial unstack conformation where Ade and Iso rings are close to each other but not in the preferably stacked conformation. U2 and U3 denote intermediate distance separation. In U2, the angle between the planes conforms to stacked geometry; however, the rings are far away (>6 Å) to have perfect stacking interactions. Variations of these parameters for FAD in water are shown in Figure S1. The time variation of the distance between Iso and Ade rings in water is shown in Figure S1a, while their distribution is shown in Figure S1d. Distribution is peaked at 4.2 Å (with 0.6 Å standard deviation). This indicates that most of the time the two rings of FAD are in close proximity. Time variations of the two angles (θ, φ) are shown in Figure S1b and S1c, while their corresponding distributions are shown in Figure S1e and S1f, respectively. It is clear from the distribution that θ is peaked at 172.1°, while φ is peaked at 143.5°. Therefore, according to the stacking criteria (as mentioned above), FAD remains in the stacked conformation most of the time in water. Unstack conformation appears for a short while for around 200 ps (Figure S1, inset). Orientation of water molecules in different possible conformations of FAD in water at different time trajectory is shown in Figure S2. It shows that a dominant number of stack conformations exist at almost all time frames, in perfect agreement with the experimental results.[9−11]

A similar analysis of FAD is carried out for FAD in a water−urea mixture (8 M). Results are shown in Figure 5. A dramatic fluctuation in FAD conformation is observed here. It is clear from the time-variation of the distance and angles that FAD prefers to exist in an unstack conformation most of the time in the mixture. However, FAD does not remain always in the unstack conformation and stack−unstack equilibrium continues. Red boxes (Figure 5) indicate the time zones where a stack conformation appeared during the simulation. Distribution of the distance (d) between the two rings exhibits (Figure 5d) distinct peaks at 4, 8, 11, and 15 Å. Interestingly, distribution of two angles θ and φ are almost uniform, which indicates that the preference for the stack conformation present in pure water is affected by urea.

The stack−unstack equilibrium is analyzed to find the probability of each conformation in both water and a water−urea mixture. Table 3 shows that 64% of FAD conformation is in stack conformation in water and the rest 36% is in unstack conformation, in close agreement with the experimental observation obtained here (Table 2). Among the unstack conformation in water, a significant portion (35.6%) comes from partial unstack conformation, U3, where the distance between two rings lies between 6 and 10 Å and the angles θ and φ are between 40 and 140°. This indicates that, in water, FAD never actually goes to the fully unstack configuration, rather the rings adopt different orientations to get out from the stacking interaction. However, from fluorescence lifetime results we have found that almost 25% molecules (excluding solvation component) exist in the unstack conformation (Table 2). The

dx.doi.org/10.1021/jp412339a | J. Phys. Chem. B 2014, 118, 1881−1890

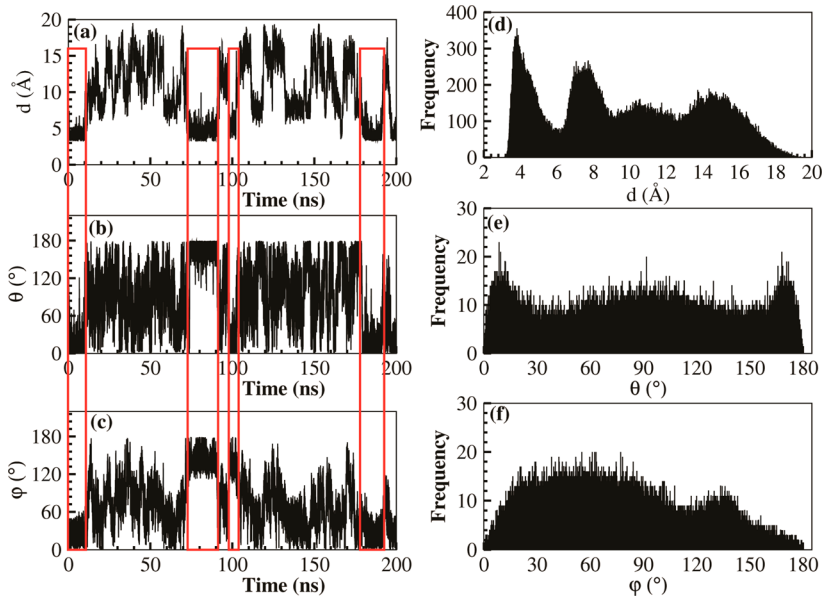

Figure 5. (a–c) Variations of the three parameters (d, θ, and φ) over trajectory. (d–f) Distribution of the above-mentioned three parameters in water–urea mixture.

Table 3. Percentage of Stack and Unstack Conformation of FAD in Water and Water–Urea Mixture Calculated over the Whole Trajectory

		unstack conformation			
solvent	stack conformation (%)	U1 (%)	U2 (%)	U3 (%)	U4 (%)
water	64	0.1	0.2	35.6	0.07
water–urea mixture (8 M)	14.4	18.4	5.4	14.5	47.3

slight discrepancy may arise by the precise definition of unstack conformations in our computational approach; whereas the population of unstack conformations obtained in experiment was from unquenched lifetime only. Also note that, the molecular dynamics simulation provides the interaction among different species in their ground electronic state only, whereas the experiment gathers this information through the excited state. However, it is not expected that the dynamical structures of isoalloxazine in the ground and excited electronic state will show significant differences, as is evident from the reasonable agreement between experiment and theory obtained here.

Amazingly, in the water–urea mixture, only 14.5% FAD molecules exist in the stack conformation, and the remaining 85% FAD molecules attains the unstack conformation (Table 3). Some representative configuration of urea molecules around FAD in stack and unstack conformations obtained at different time frames are shown in Figure 6. Among the total population of unstack conformation, a majority of the structure exists in the completely unstack conformation U4 (47.3%), where the distance between the two rings is more than 10 Å. The partially unstack conformation contains all the three possibilities (U1, U2, and U3) discussed previously. A total of 18.4% of structures contain two rings close to each other with unfavorable stacking orientation (U1), while 5.4% of structures are of U2 type, where angles are of the stacking type, but the distance between the rings does not allow stacking interaction. The remaining 14.5% of structures exist in U3 conformation, where both the distance and the angles do not allow stacking to

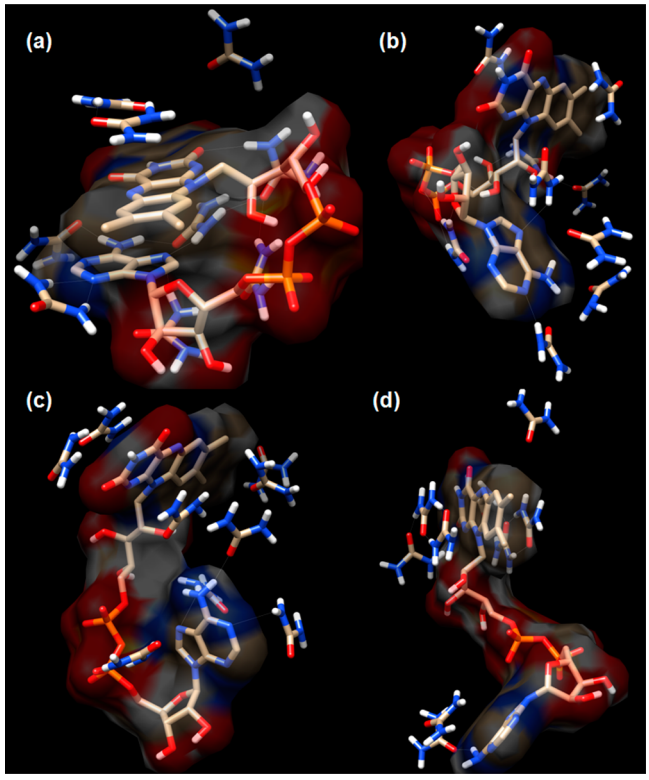

Figure 6. Orientations of urea molecules around isoalloxazine and adenine rings of FAD at different time points in the trajectory.

occur. Although the above results support our claim that the contribution of unstack conformations increases in presence of urea, we cannot correlate the exact population of stack and unstack conformations obtained from simulation with experiments. This is because, in experiment, a significant portion of the decay profile contains solvation component, which cannot be detected in simulation as it is done in the ground state. Moreover, in the experiment we have identified the stack conformations through the quenched lifetime of FAD, and here

dx.doi.org/10.1021/jp412339a | J. Phys. Chem. B 2014, 118, 1881–1890

the total population of stack conformations of FAD is a combination of A_2 and A_3. In simulation, on the other hand, we have defined stack conformation, which fulfill the angle and distance criteria (discussed previously); all other conformations were considered as unstack.

Hydrogen-Bond Analysis. To understand the effect of water and urea on FAD conformation, we analyzed hydrogen bonds (HBs) between different parts of the FAD (Ade, Ribose (Rib), Iso rings, and phosphate groups (Phos)), and with the solvent molecules (water and urea). HB was determined by defining a distance and an angle cutoff. Distance cutoff between the donor and acceptor was taken as 3.5 Å, while the cutoff for the angle formed by the donor, hydrogen, and acceptor was taken to be 30°.[55−57]Average HBs between different parts of FAD and with solvents are shown in Figure 7. HBs between

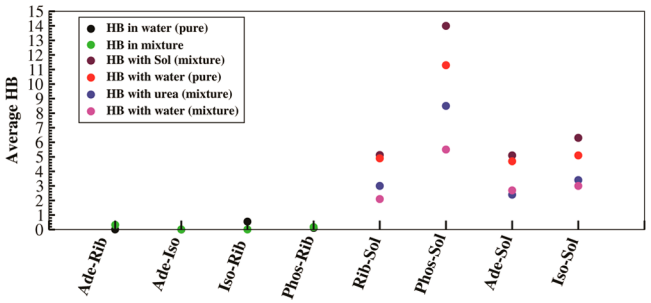

Figure 7. Average hydrogen bonding (HB) of the different parts of FAD and with the solvent (water and water−urea mixture). The black point is the average HB in the water solvent. The green point is the average HB in the water−urea mixture (8 M).

different parts of FAD (Ade, Iso, Rib, and Phos; intramolecular HBs) is almost nonexistent in water, which is consistent with the simulation results reported by Radoszkowicz et al.[18] In urea−water mixture, number of HBs between different parts of FAD is also negligibly small. The number of HBs between different parts of FAD and the solvent molecules in general is similar in the case of pure water and the mixture (Figure 7). Interestingly, in the mixture, some of the water molecules get replaced by urea for making HBs with different parts of FAD, as shown in Figure 7. Phosphate (Phos) makes maximum HBs with water in pure solvent (11.3). However, in the urea−water mixture, on an average 5.5 water molecules and 8.5 urea molecules make HBs with the phosphate group. Similarly, an average number of HBs of Ade and Iso with water in pure water is 4.7 and 5.1, respectively. This changes to 2.7 and 2.9 in the mixture, whereas average HBs of Ade and Iso with urea in the mixture is 2.4 and 3.4, respectively. Therefore, the simulation results suggest that a hydrogen bond is not the major driving factor toward the stack to unstack dominance in the presence of urea.

Structural Arrangement of Urea around FAD. To see the effect of urea on the FAD conformation, we have monitored the stack-unstack behavior of urea with Ade and Iso ring by using three parameters: (i) distance k, between the COM of Ade/Iso to the urea molecule (magnitude of vector $\vec{k}$ in Figure 4f), (ii) angle α, between the vector normal to the Ade or Iso ring and the vector normal to the urea molecule (angle between the unit vector $\hat{n}$ and $\hat{h}$ in Figure 4f), (iii) angle β, between the vector normal to the Ade or Iso ring and the vector from the COM of Ade or Iso to the urea molecule (angle between the vector $\vec{k}$ and $\hat{h}$ in Figure 4). To define the normal vector of the urea, we took the cross product of the two vectors $\hat{l}$ and $\hat{m}$, as shown in Figure 4h. Figure S3 shows the distribution of the above distance and angles of urea with the Ade/Iso rings in the urea−water mixture. Distribution of urea molecules around the rings exhibits two peaks. We defined the stack conformation, when $k \leq 5.2$ Å and $40° \geq \{\alpha, \beta\}$ or $\{\alpha, \beta\} \geq 140°$. The rest of the structural arrangements between the urea and Ade/Iso are defined as unstack conformation. We classified the unstack conformation into two types: (i) Un1 for $40° \leq \alpha$ or $\alpha \leq 140°$ and $40° \geq \beta$ or $\beta \geq 140°$. (iii) Un2 for $40° \geq \alpha$ or $\alpha \geq 140°$ and any β value. From the above definition, we can see that Un1 denotes urea configuration where the plane of the urea molecule is perpendicular to the ring plane. Un2 denotes the configuration, where urea molecules surround the ring in the periphery.

From the distribution of the distance of urea from both the above rings, we assign the cutoff distance at 5.2 Å for direct interaction of urea with the rings. Subsequently, we have analyzed the conformation of the urea in proximity of the rings from the above-mentioned criteria. Table 4 shows the number

Table 4. Percentage of Stack and Unstack Conformation of Urea with Both Ring Ade and Iso

	cut-off distance (Å)	number of urea molecule	% stack	% unstack	
				Un1	Un2
Ade	5.2	2.6	28.4	15.0	56.4
Iso	5.2	3.0	39.0	11.7	48.5

of urea molecules around the Ade and Iso in both stack and unstack conformation. We have found that, on average, 2.6 urea molecules are within 5.2 Å distance from the Ade ring and 3 urea molecules are within 5.2 Å distance from the Iso ring. Orientation of the urea molecules around the Ade and Iso rings is different as mentioned in Table 4. A total of 39% of the urea molecules around the Iso ring form stack conformation, whereas 28.4% urea molecules stack around Ade. In unstack conformation, a majority of the conformation exists in Un2 conformation for both the rings, and these urea molecules participate in hydrogen bond interactions with rings.

From the analysis of the structural arrangement of urea around FAD, we have observed that, in the mixture, urea replaces water to interact with different parts of the ring. Although the overall number of hydrogen bonds between FAD and the solvent does not change from the pure water to the mixture, urea replaces some of the water molecules from both of the rings to participate in stacking and hydrogen bonding interactions with Ade and Iso rings. Moreover, participation of urea around Ade and Iso is more when FAD is in unstack conformation. Number of urea around Ade and Iso is 2.0 in stack conformation, while the number of urea around Ade is 2.9 and around Iso is 3.5 in the unstack geometry. This participation comes partially (∼30−40%) from the stacking interaction of urea with Ade/Iso rings. This decreases the probability of FAD to be in the stack conformation in the presence of urea, thereby shifting the equilibrium toward more unstack conformations.

■ CONCLUSION

Present work focuses on the urea induced unfolding of FAD through steady state, femto to nanosecond, time-resolved fluorescence spectroscopy, and molecular dynamics simulation

dx.doi.org/10.1021/jp412339a | J. Phys. Chem. B 2014, 118, 1881−1890

studies. It is evident from steady state emission profiles that the intensity of FAD rises up with increasing urea concentration. A comparative study with FMN exhibits a small decrement in intensity. As stack conformation is almost nonfluorescent in nature, the above observation suggests that the population of unstack conformation increases in the presence of urea. The fluorescence decay profiles collected in both TCSPC and up-conversion techniques slow down in the presence of urea, indicating a significant change in the stack−unstack dynamics of FAD in presence of urea. Moreover, it is observed that the unstack conformation population increases from 15% in pure water to 40% in 12 M urea. Results obtained from molecular dynamics simulation support this observation very well. It shows that although the total number of hydrogen bonds remains same in water and urea−water mixture, urea replaces many of the water molecules around adenine and isoalloxazine rings of FAD. Moreover, MD simulation studies reveal that a major fraction of urea molecules (∼30−40%) involves in stacking interactions with both of the adenine and isoalloxazine rings. As a result, intramolecular stacking interaction between the isoalloxazine and adenine rings is disrupted, and thereby, the contribution of the unstack conformation of FAD increases with increasing urea concentration in the medium.

■ ASSOCIATED CONTENT

Supporting Information

Additional supporting figures. This material is available free of charge via the Internet at http://pubs.acs.org.

■ AUTHOR INFORMATION

Corresponding Author

*E-mail: arnab.mukherjee@iiserpune.ac.in; p.hazra@iiserpune.ac.in. Tel.: +91-20-2590-8077 (P.H.); +91-20-2590-8051 (A.M.). Fax: +91-20-2589 9790 (P.H.).

Author Contributions

†These authors contributed equally to this work (A.S. and R.K.S.).

Notes

The authors declare no competing financial interest.

■ ACKNOWLEDGMENTS

P.H. thanks to Council of Scientific and Industrial Research (CSIR), Government of India, for partial financial support. A.M. is indebted to DST (DST Project SB/S1/PC-39/2012 and DST Nanomission SR/NM/MS-15/2011) for partial financial support. A.S. is thankful to CSIR for Senior Research Fellowship (SRF). R.K.S. and R.K.K. are thankful to University Grants Commission (UGC) for Junior Research Fellowships (JRF). Authors thank Director, IISER-Pune, for providing excellent experimental and computation facilities. Authors are indebted to anonymous reviewers for their valuable suggestions.

■ REFERENCES

(1) van der Horst, M. A.; Hellingwerf, K. J. Photoreceptor Proteins, "Star Actors of Modern Times": A Review of the Functional Dynamics in the Structure of Representative Members of Six Different Photoreceptor Families. *Acc. Chem. Res.* **2003**, *37*, 13−20.

(2) Ghisla, S.; Kroneck, P.; Macheroux, P.; Sund, H. *Flavins and Flavoproteins*; Rudolf-Weber Agency for Scientific Publications: Berlin, 1999.

(3) Kao, Y.-T.; Saxena, C.; He, T.-F.; Guo, L.; Wang, L.; Sancar, A.; Zhong, D. Ultrafast Dynamics of Flavins in Five Redox States. *J. Am. Chem. Soc.* **2008**, *130*, 13132−13139.

(4) Müller, F. The Flavin Redox-System and its Biological Function. *Radicals in Biochemistry*; Springer: Berlin, Heidelberg, 1983; Vol. *108*, pp 71−107.

(5) Begley, T. P. Photoenzymes: A Novel Class of Biological Catalysts. *Acc. Chem. Res.* **1994**, *27*, 394−401.

(6) Iseki, M.; Matsunaga, S.; Murakami, A.; Ohno, K.; Shiga, K.; Yoshida, K.; Sugai, M.; Takahashi, T.; Hori, T.; Watanabe, M. A Blue-Light-Activated Adenylyl Cyclase Mediates Photoavoidance in *Euglena gracilis*. *Nature* **2002**, *415*, 1047−1051.

(7) Huang, Y.; Baxter, R.; Smith, B. S.; Partch, C. L.; Colbert, C. L.; Deisenhofer, J. Crystal Structure of Cryptochrome 3 from *Arabidopsis thaliana* and its Implications for Photolyase Activity. *Proc. Natl. Acad. Sci. U.S.A.* **2006**, *103*, 17701−17706.

(8) Sancar, A. Structure and Function of DNA Photolyase and Cryptochrome Blue-Light Photoreceptors. *Chem. Rev.* **2003**, *103*, 2203−2238.

(9) Weber, G. Fluorescence of Riboflavin and Flavin-Adenine Dinucleotide. *Biochem. J.* **1950**, *47*, 114−121.

(10) Sengupta, A.; Khade, R. V.; Hazra, P. pH Dependent Dynamic Behavior of Flavin Mononucleotide (FMN) and Flavin Adenine Dinucleotide (FAD) in Femtosecond to Nanosecond Time Scale. *J. Photochem. Photobiol., A* **2011**, *221*, 105−112.

(11) van den Berg, P. A. W.; Feenstra, K. A.; Mark, A. E.; Berendsen, H. J. C.; Visser, A. J. W. G. Dynamic Conformations of Flavin Adenine Dinucleotide: Simulated Molecular Dynamics of the Flavin Cofactor Related to the Time-Resolved Fluorescence Characteristics. *J. Phys. Chem. B* **2002**, *106*, 8858−8869.

(12) Islam, S. D. M.; Susdorf, T.; Penzkofer, A.; Hegemann, P. Fluorescence Quenching of Flavin Adenine Dinucleotide in Aqueous Solution by pH Dependent Isomerisation and Photo-Induced Electron Transfer. *Chem. Phys.* **2003**, *295*, 137−149.

(13) Chosrowjan, H.; Taniguchi, S.; Mataga, N.; Tanaka, F.; Visser, A. J. W. G. The Stacked Flavin Adenine Dinucleotide Conformation in Water is Fluorescent on Picosecond Timescale. *Chem. Phys. Lett.* **2003**, *378*, 354−358.

(14) Li, G.; Glusac, K. D. Light-Triggered Proton and Electron Transfer in Flavin Cofactors. *J. Phys. Chem. A* **2008**, *112*, 4573−4583.

(15) Li, G.; Glusac, K. D. The Role of Adenine in Fast Excited-State Deactivation of FAD: a Femtosecond Mid-IR Transient Absorption Study. *J. Phys. Chem. B* **2009**, *113*, 9059−9061.

(16) Stanley, R. J. MacFarlane Ultrafast Excited State Dynamics of Oxidized Flavins: Direct Observations of Quenching by Purines. *J. Phys. Chem. A* **2000**, *104*, 6899−6906.

(17) Weigel, A.; Dobryakov, A.; Klaumünzer, B.; Sajadi, M.; Saalfrank, P.; Ernsting, N. P. Femtosecond Stimulated Raman Spectroscopy of Flavin after Optical Excitation. *J. Phys. Chem. B* **2011**, *115*, 3656−3680.

(18) Radoszkowicz, L.; Huppert, D.; Nachliel, E.; Gutman, M. Sampling the Conformation Space of FAD in Water−Methanol Mixtures through Molecular Dynamics and Fluorescence Measurements. *J. Phys. Chem. A* **2009**, *114*, 1017−1022.

(19) Radoszkowicz, L.; Presiado, I.; Erez, Y.; Nachliel, E.; Huppert, D.; Gutman, M. Time-Resolved Emission of Flavin Adenine Dinucleotide in Water and Water−Methanol Mixtures. *Phys. Chem. Chem. Phys.* **2011**, *13*, 12058−12066.

(20) Nakabayashi, T.; Islam, M. S.; Ohta, N. Fluorescence Decay Dynamics of Flavin Adenine Dinucleotide in a Mixture of Alcohol and Water in the Femtosecond and Nanosecond Time Range. *J. Phys. Chem. B* **2010**, *114*, 15254−15260.

(21) Sengupta, A.; Gavvala, K.; Koninti, R. K.; Chaudhuri, H.; Hazra, P. Folding Dynamics of Flavin Adenine Dinucleotide (FAD) inside Nonaqueous and Aqueous Reverse Micelles. *Chem. Phys. Lett.* **2013**, *584*, 67−73.

(22) Hoccart, X.; Turrell, G. Raman Spectroscopic Investigation of the Dynamics of Urea−Water Complexes. *J. Chem. Phys.* **1993**, *99*, 8498−8503.

(23) Finer, E. G.; Franks, F.; Tait, M. J. Nuclear Magnetic Resonance Studies of Aqueous Urea Solutions. *J. Am. Chem. Soc.* **1972**, *94*, 4424−4429.

(24) Hammes, G. G.; Schimmel, P. R. An Investigation of Water–Urea and Water–Urea–Polyethylene Glycol Interactions. *J. Am. Chem. Soc.* **1967**, *89*, 442–446.
(25) Funkner, S.; Havenith, M.; Schwaab, G. Urea, a Structure Breaker? Answers from THz Absorption Spectroscopy. *J. Phys. Chem. B* **2012**, *116*, 13374–13380.
(26) Guinn, E. J.; Pegram, L. M.; Capp, M. W.; Pollock, M. N.; Record, M. T. Quantifying Why Urea is a Protein Denaturant, Whereas Glycine Betaine is a Protein Stabilizer. *Proc. Natl. Acad. Sci. U.S.A.* **2011**, *108*, 16932–16937.
(27) Kauzmann, W.; Simpson, R. B. The Kinetics of Protein Denaturation. III. The Optical Rotations of Serum Albumin, β-Lactoglobulin and Pepsin in Urea Solutions. *J. Am. Chem. Soc.* **1953**, *75*, 5154–5157.
(28) Canchi, D. R.; Paschek, D.; García, A. E. Equilibrium Study of Protein Denaturation by Urea. *J. Am. Chem. Soc.* **2010**, *132*, 2338–2344.
(29) Sengupta, A.; Sasikala, W. D.; Mukherjee, A.; Hazra, P. Comparative Study of Flavins Binding with Human Serum Albumin: A Fluorometric, Thermodynamic, and Molecular Dynamics Approach. *ChemPhysChem* **2012**, *13*, 2142–2153.
(30) Gavvala, K.; Sengupta, A.; Hazra, P. Modulation of Photophysics and pKa Shift of the Anti-Cancer Drug Camptothecin in the Nanocavities of Supramolecular Hosts. *ChemPhysChem* **2013**, *14*, 532–542.
(31) Gavvala, K.; Sengupta, A.; Koninti, R. K.; Hazra, P. Prototropical and Photophysical Properties of Ellipticine inside the Nanocavities of Molecular Containers. *J. Phys. Chem. B* **2013**, *117*, 14099–14107.
(32) Gavvala, K.; Sengupta, A.; Koninti, R. K.; Hazra, P. Supramolecular Host-Inhibited Excited-State Proton Transfer and Fluorescence Switching of the Anti-Cancer Drug, Topotecan. *ChemPhysChem* **2013**, *14*, 3375–3383.
(33) Gavvala, K.; Sengupta, A.; Koninti, R. K.; Hazra, P. Femtosecond to Nanosecond Dynamics of 2,2′-Bipyridine-3,3′-Diol inside the Nano-Cavities of Molecular Containers. *Phys. Chem. Chem. Phys.* **2014**, *16*, 933–939.
(34) Frisch, M. J.; Trucks, G. W.; Schlegel, H. B.; Scuseria, G. E.; Robb, M. A.; Cheeseman, J. R.; Scalmani, G.; Barone, V.; Mennucci, B.; Petersson, G. A.; et al. *Gaussian 09*, rev. A.02; Gaussian, Inc.: Wallingford, CT, 2009.
(35) Case, D. A.; Cheatham, T. E.; Darden, T.; Gohlke, H.; Luo, R.; Merz, K. M.; Onufriev, A.; Simmerling, C.; Wang, B.; Woods, R. J. The Amber Biomolecular Simulation Programs. *J. Comput. Chem.* **2005**, *26*, 1668–1688.
(36) Cornell, W. D.; Cieplak, P.; Bayly, C. I.; Kollmann, P. A. Application of RESP Charges to Calculate Conformational Energies, Hydrogen Bond Energies, and Free Energies of Solvation. *J. Am. Chem. Soc.* **1993**, *115*, 9620–9631.
(37) Wang, J.; Wolf, R. M.; Caldwell, J. W.; Kollman, P. A.; Case, D. A. Development and Testing of a General Amber Force Field. *J. Comput. Chem.* **2004**, *25*, 1157–1174.
(38) Sorin, E. J.; Pande, V. S. Exploring the Helix-Coil Transition via All-Atom Equilibrium Ensemble Simulations. *Biophys. J.* **2005**, *88*, 2472–2493.
(39) Jorgensen, W. L.; Chandrasekhar, J.; Madura, J. D.; Impey, R. W.; Klein, M. L. Comparison of Simple Potential Functions for Simulating Liquid Water. *J. Chem. Phys.* **1983**, *79*, 926–935.
(40) Hess, B.; Kutzner, C.; van der Spoel, D.; Lindahl, E. GROMACS 4: Algorithms for Highly Efficient, Load-Balanced, and Scalable Molecular Simulation. *J. Chem. Theor. Comput.* **2008**, *4*, 435–447.
(41) Press, W. H.; Teukolsky, S. A.; Vetterling, W. T.; Flannery, B. P. *Numerical Recipes: The Art of Scientific Computing*, 3rd ed.; Cambridge University Press: U.K., 2007; p 1256.
(42) Berendsen, H. J. C.; Postma, J. P. M.; van Gunsteren, W. F.; DiNola, A.; Haak, J. R. Molecular Dynamics with Coupling to an External Bath. *J. Chem. Phys.* **1984**, *81*, 3684–3690.
(43) Hess, B.; Bekker, H.; Berendsen, H. J. C.; Fraaije, J. G. E. M. LINCS: A Linear Constraint Solver for Molecular Simulations. *J. Comput. Chem.* **1997**, *18*, 1463–1472.
(44) Darden, T.; York, D.; Pedersen, L. Particle Mesh Ewald: An *N* log(*N*) Method for Ewald Sums in Large Systems. *J. Chem. Phys.* **1993**, *98*, 10089–10092.
(45) Nosé, S. A Molecular Dynamics Method for Simulations in the Canonical Ensemble. *Mol. Phys.* **1984**, *52*, 255–268.
(46) Parrinello, M.; Rahman, A. Polymorphic Transitions in Single Crystals: A New Molecular Dynamics Method. *J. Appl. Phys.* **1981**, *52*, 7182–7190.
(47) Drössler, P.; Holzer, W.; Penzkofer, A.; Hegemann, P. pH Dependence of the Absorption and Emission Behaviour of Riboflavin in Aqueous Solution. *Chem. Phys.* **2002**, *282*, 429–439.
(48) Wyman, J. Dielectric Constants: Ethanol—Diethyl Ether and Urea—Water Solutions between 0 and 50°. *J. Am. Chem. Soc.* **1933**, *55*, 4116–4121.
(49) Walrafen, G. E. Raman Spectral Studies of the Effects of Urea and Sucrose on Water Structure. *J. Chem. Phys.* **1966**, *44*, 3726–3727.
(50) Mazur, K.; Heisler, I. A.; Meech, S. R. THz Spectra and Dynamics of Aqueous Solutions Studied by the Ultrafast Optical Kerr Effect. *J. Phys. Chem. B* **2011**, *115*, 2563–2573.
(51) Seidel, C. A. M.; Schulz, A.; Sauer, M. H. M. Nucleobase-Specific Quenching of Fluorescent Dyes. 1. Nucleobase One-Electron Redox Potentials and Their Correlation with Static and Dynamic Quenching Efficiencies. *J. Phys. Chem.* **1996**, *100*, 5541–5553.
(52) Draper, R. D.; Ingraham, L. L. A Potentiometric Study of the Flavin Semiquinone Equilibrium. *Arch. Biochem. Biophys.* **1968**, *125*, 802–808.
(53) Hayashi, Y.; Katsumoto, Y.; Omori, S.; Kishii, N.; Yasuda, A. Liquid Structure of the Urea–Water System Studied by Dielectric Spectroscopy. *J. Phys. Chem. B* **2007**, *111*, 1076–1080.
(54) Guinn, E. J.; Schwinefus, J. J.; Cha, H. K.; McDevitt, J. L.; Merker, W. E.; Ritzer, R.; Muth, G. W.; Engelsgjerd, S. W.; Mangold, K. E.; Thompson, P. J.; Kerins, M. J.; Record, M. T. Quantifying Functional Group Interactions that Determine Urea Effects on Nucleic Acid Helix Formation. *J. Am. Chem. Soc.* **2013**, *135*, 5828–5838.
(55) Luzar, A.; Chandler, D. Hydrogen-Bond Kinetics in Liquid Water. *Nature* **1996**, *379*, 55–57.
(56) van der Spoel, D.; van Maaren, P. J.; Larsson, P.; Tîmneanu, N. Thermodynamics of Hydrogen Bonding in Hydrophilic and Hydrophobic Media. *J. Phys. Chem. B* **2006**, *110*, 4393–4398.
(57) Luzar, A. Resolving the Hydrogen Bond Dynamics Conundrum. *J. Chem. Phys.* **2000**, *113*, 10663–10675.